How can we effectively evaluate a reentry forecast to ensure its accuracy and reliability?

Szücs-Csillik, I.[1], De Cicco, M.[2], Turcu, V.[1]

[1]Romanian Academy, Astronomical Institute, Astronomical Observatory Cluj-Napoca
[2]INMETRO - National Institute of Metrology, Quality and Technology, Brazil
Exoss project, press.exoss.org
iharkagmail.com, decicco10@gmail.com, vladturcu@yahoo.com

Abstract

The predictability of artificial satellite reentries has significantly improved in recent years. A notable example occurred on May 10, 2025, at 6:40 UTC (with a margin of ± 1.5 hours): the uncontrolled reentry of the Kosmos 482 Descent Craft (1972-023E). This object dates back to 1972 and was a lander module that failed during the Soviet Venera mission to Venus. Due to a malfunction of the rocket's upper stage, it became trapped in a highly elliptical orbit around Earth instead of heading toward Venus. According to the literature, the object was approximately 1 meter in size and had a semi-spherical shape, with a mass of 495 kg. It was designed to withstand the intense conditions of the Venusian atmosphere, which makes the potential risk of impact significant. Using the reentry model developed by Szücs-Csillik (2017), we analyzed the orbital evolution and behavior of Kosmos 482 leading up to its reentry and compared our predictions with other estimates. After the reentry of Kosmos 482, we assessed the existing forecasts and refined our model. With each reentry, we enhance our understanding and improve our predictive capabilities.

1. Introduction

From the historic first space launch on October 4, 1957, to the year 2025, an astounding quantity of metric tons of man-made objects has been launched into orbit around the Earth, the Sun, and other celestial bodies.

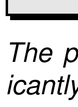

An increasing quantity of artificial objects is reentering the Earth's atmosphere, mainly comprising space debris, as well as mission-related materials and intact spacecraft such as satellites and rocket bodies.
The study of close approaches (collisions) between minor and major celestial bodies reveals important dynamics in our solar system. For instance, any minor body that reaches perihelion inside Earth's orbit can approach unnoticed, concealed in the daytime sky. When the minimum approach distance from Earth is less than 0.001 AU, known as the Red Baron dynamic scenario, and the object is obscured by the glare of the Sun, it poses a significant risk for a very close encounter or even an impact. A prominent example of this occurred with the Chelyabinsk meteor on February 15, 2013.

2. Dynamical model

The motion of a satellite is influenced by various forces that shape its trajectory. The most significant of these is the force of gravitation, primarily resulting from Earth's attraction. For this reason, we consider the Earth's gravitational potential terms up to $c40$ for zonal harmonics and $c31$, $s31$ for tesseral harmonics.
Another major factor affecting an artificial satellite near Earth is atmospheric drag. This drag causes the perigee distance of the satellite to change more slowly than the apogee distance, leading the orbit to gradually take on a more circular shape. In our analysis, we focused on the simplest form of atmospheric drag perturbation. Other factors affecting the artificial satellite include the gravitational influences of the sun and moon, as well as solar radiation pressure and solar cycle effects (Oliveira et al. 2025).
The precise orbit prediction of the artificial satellite's motion depends on correct initial conditions and on an adequate numerical integrator (Szücs-Csillik, Turcu 2023).

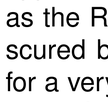

Let's consider an Earth-centered, Earth-fixed (ECEF) coordinate system with axes x, y, and z. We will examine how the oblateness of the Earth and atmospheric drag affect satellite motion. The differential equations governing satellite motion in rectangular coordinates are expressed in the following form:

$$\begin{aligned} \frac{d^2x}{dt^2} &= \frac{\partial U}{\partial x}, \\ \frac{d^2y}{dt^2} &= \frac{\partial U}{\partial y}, \\ \frac{d^2z}{dt^2} &= \frac{\partial U}{\partial z}, \end{aligned} \tag{1}$$

$$U = U_{00}+U_{20}+U_{22}+U_{30}+U_{31}+U_{40}+U_A, \tag{2}$$

$$\begin{aligned} U_{00} &= \frac{\mu}{r}, \\ U_{20} &= \frac{1}{2}\mu R^2 c_{20}\cdot\left(\frac{3z^2}{r^5}-\frac{1}{r^3}\right), \\ U_{22} &= 3\mu R^2\left[\left(\frac{x^2-y^2}{r^5}c_{22}+\frac{2xy}{r^5}s_{22}\right)\cos 2s + \right. \\ &+ \left.\left(\frac{2xy}{r^5}c_{22}-\frac{x^2-y^2}{r^5}s_{22}\right)\sin 2s\right] \\ U_{30} &= \frac{1}{2}\mu R^3 c_{30}\cdot\left(\frac{5z^3}{r^7}-\frac{2z}{r^5}\right), \\ U_{31} &= \frac{3}{2}\mu R^3\left[\left(\left(\frac{5xz^2}{r^7}-\frac{x}{r^5}\right)c_{31}+\left(\frac{5yz^2}{r^7}-\frac{y}{r^5}\right)s_{31}\right)\cos s + \right. \\ &+ \left.\left(\left(\frac{5yz^2}{r^7}-\frac{y}{r^5}\right)c_{31}-\left(\frac{5xz^2}{r^7}-\frac{x}{r^5}\right)s_{31}\right)\sin s\right] \\ U_{40} &= \frac{1}{8}\mu R^4 c_{40}\cdot\left(\frac{35z^4}{r^9}-\frac{30z^2}{r^7}+\frac{3}{r^5}\right), \\ U_A &= -\frac{1}{2}\frac{\rho C_D A}{m}v_r v_r, \end{aligned} \tag{3}$$

where μ is the gravity constant, r is the distance from the center of mass, R is the equatorial radius of the Earth, s is the argument of latitude, and ρ is the atmospheric density, C_D is the drag coefficient, A is the cross-sectional area of the satellite perpendicular to the velocity vector, m is the mass of the satellite, and v_r is the satellite velocity vector relative to the atmosphere.

3. Numerical integrator

Symplectic integrators are essential tools in the field of celestial mechanics. They provide two significant advantages over most other algorithms. First, they completely eliminate the long-term accumulation of energy error, ensuring greater accuracy over time. Second, these integrators allow for the seamless incorporation of each object's motion around the central body, which means that the step size can be effectively determined by the smaller perturbations between the bodies, rather than the dominant forces from the central body. Third, symplectic integration methods possess a certain backward stability characteristic.
We used Neri's fourth-order symplectic integrator (Szücs-Csillik 2010, De Cicco and Szücs-Csillik 2024) to simulate backward the dynamics of the close approach.
By employing the two-line elements—including the semi-major axis (a), eccentricity (e), inclination (i), right ascension of the ascending node (Ω), argument of perigee (ω), mean anomaly (M), the $BSTAR$ drag coefficient, and the epoch (t), we conducted a thorough numerical investigation into the dynamic trajectories of some satellites and meteoroids. The results of our selected analysis can be seen in Figures 1b and 2b.

4. Applications

4.1 Kosmos 482

This mission Kosmos 482 (Launch Date: 1972-03-31, Launch Site: Tyuratam, Mass: 1184 kg) was an attempted Venus probe which failed to escape low Earth orbit. It was launched by an SL-6/A-2-e launcher 4 days after the Venera 8 atmospheric probe and had an identical design and mission plan.

The Kosmos 482 lander probe (1972-023E) reentered Earth's atmosphere on May 10 at 06:24 UT over the Indian Ocean. Because the probe was designed to withstand entry into the Venus atmosphere, it is possible it survived reentry but has landed in the ocean west of Jakarta, Indonesia.
Our reentry simulation indicates a decrease in the satellite's altitude over the past 360 minutes (Figure 1).

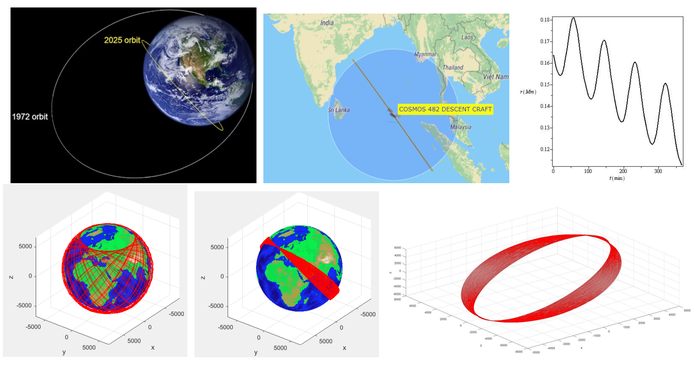

Figure 1: *a. Reentry location (credit: satflare.com); b. Reentry prediction (360 min) with the model of Szücs-Csillik (2017) from the Last TLE epoch 2025.05.10, 0:35:55 UTC.; c. Calculated ECEF orbit before reentry around the Earth; d. Calculated ECI orbit before reentry around the Earth; e. Modeled ECI orbit before reentry. *We trace the satellite's state vector back 5 days, and the continents do not align with the orbit.*

4.2 Starlink 32563

Starlink 32563 (Launch Date: 2025-03-26, Launch Site: Vandenberg AFB, Mass: 730 kg) is the second of twenty-seven V2-mini satellites that comprise Starlink Group 11-7.

This satellite orbits about 550 km above Earth and can hinder optical and radio astronomical observations.
Our reentry simulation illustrates the fluctuations in the satellite's altitude over the past 900 minutes (Figure 2).

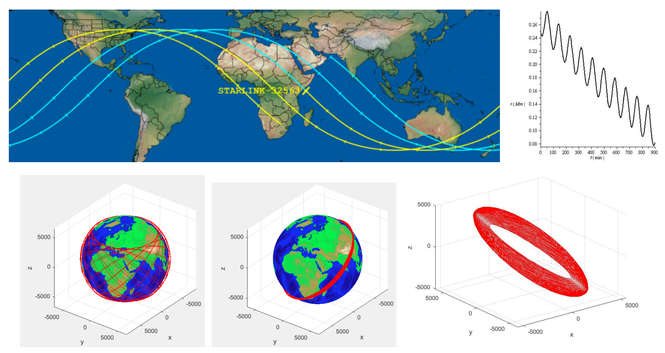

Figure 2: *a. Reentry location (Credit: aerospace.org); b. Reentry prediction from 2025.06.02 4:32:26.863 UTC (last TLE) is around 900 minutes = 15h; c. Calculated ECEF orbit before reentry; d. Calculated ECI orbit before reentry - around the Earth; e. Modeled ECI orbit before reentry (3 days).*

A reentry was observed from São Luis, Brazil on 2025.06.02 at 22:03:40 UTC. The Aerospace forecasted the reentry windows to be on June 2, 2025, at 19:32 UTC ± 3 hours (Figure 3).

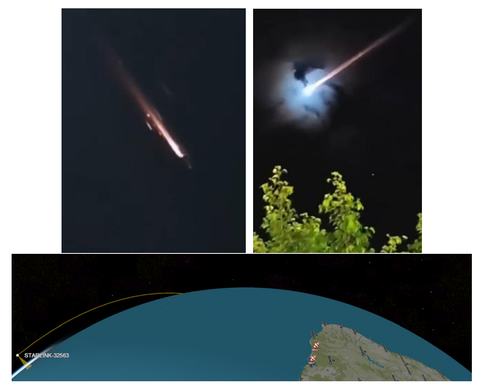

Figure 3: *a. Unidentified object scares residents in Santo Amaro do Maranhao; b. Modeled orbit of Starlink 32543 (Credit: satvis.space).*

The date and time align with the observations and reentry predictions. However, a closer look reveals that the object originated from a different direction than that of the *Starlink 32543*. Thus, even though the time and location coincide, the object observed is actually a meteoroid.

5. Results and discussions

The challenge of predicting the reentry of small celestial objects into our atmosphere is both complex and increasingly urgent. Addressing this need is essential for our understanding and preparedness in the face of these cosmic events.
Research on various satellite reentries indicates that the target perigee altitude for such reentries is roughly between 100 and 150 km. Upon reaching this designated altitude, a satellite will impact the Earth after a duration of around 1000 seconds. It is important to note that the timing of the reentry is also influenced by local conditions, including atmospheric factors and terrain elevation.
To effectively evaluate a reentry forecast, it is essential to ensure its accuracy and reliability.

6. Selected references

1. De Cicco, M., Szücs-Csillik, I.: 2024, *Published by the International Meteor Organization*, 64.
2. Oliveira, D. M., et al.: 2025, *Front. Astron. Space Sci.* **12**, 1572313.
3. Szücs-Csillik, I.: 2010, *Rom. Astron. J.* **20**, 49.
4. Szücs-Csillik, I.: 2017, *Rom. Astron. J.* **27**, 241.
5. Szücs-Csillik, I., Turcu, V.: 2023, *7th International Conference in Astronomy, Astrophysics, Space and Planetary Sciences*, 10-12 July 2023, Cluj-Napoca, Romania.